

Fast-decaying inductive IP in frozen ground

N.O. Kozhevnikov *

A.A. Trofimuk Institute of Petroleum Geology and Geophysics, Siberian Branch of the Russian Academy of Sciences,
pr. Akademika Koptuyuga 3, Novosibirsk, 630090, Russia

Received 2 September 2010; accepted 5 April 2011

Abstract

Effects of induced polarization (IP) often appear in TEM data collected in Yakutia and elsewhere in permafrost areas. Inversion of transient responses using the Cole–Cole model of frequency-dependent conductivity shows fast decaying induced polarization in the shallow subsurface (within 100 m). Frozen ground within these depths has the chargeability (m) in the range from 0.2 to 0.85 (mostly 0.2–0.5); the relaxation time constant (τ) varies from 35 to 250 μ s being 50–100 μ s on average, and the exponent c is little variable, unlike m and τ (from 0.8 to 1). The latter fact ($c \approx 1$) is indicative of a narrow range of relaxation times fitting the Debye relaxation model. Conversion of the complex conductivity into relative low-frequency dielectric permittivity results in values of the order of tens of thousands or a few hundred thousand. These exceptionally high permittivities have no other plausible explanations than electrochemical polarization of unfrozen water that remains bound on the surface of mineral grains at subzero temperatures. The effects of electrochemical polarization are described and interpreted in terms of frequency-dependent surface conductivity, which is controlled by surface-to-volume ratio.

© 2012, V.S. Sobolev IGM, Siberian Branch of the RAS. Published by Elsevier B.V. All rights reserved.

Keywords: TEM surveys; induced polarization; frozen ground; ice; low-frequency dielectric permittivity; Maxwell–Wagner effect; electrochemical polarization; surface conductance

Introduction

Transient responses measured in areas of permafrost (Yakutia, Canada, Alaska) often show break in monotony or even sign reversals. These effects result from fast decaying induced polarization (Kozhevnikov and Antonov, 2006, 2009a,b; Krylov and Bobrov, 2002; Molchanov and Sidorov, 1985; Sidorov, 1985, 1987; Smith and Klein, 1996; Stognii, 2008; Stognii and Korotkov, 2010; Vanchugov and Kozhevnikov, 1998; Walker and Kawasaki, 1988). In frequency-domain the IP effects show up as frequency dependence of conductivity and/or dielectric permittivity of rocks.

TEM data affected by induced polarization are not restricted uniquely to cold regions, but it is in areas of permafrost that they are persistent. For instance, thousands or maybe tens of thousands of IP affected transients were collected in Yakutia. There are reasons to attribute fast decaying polarization to ion-conducting rather than to electron-conductance mechanisms which are unlikely in frozen rocks (Kozhevnikov and Antonov, 2009b, 2010; Olenchenko et al., 2008).

Explicit evidence that the same rocks *in situ*, produce IP-affected transient responses when they are frozen but are not polarizable in the unfrozen state was obtained in 1992 in northern Buryatia, near Taksimo Village (Kozhevnikov et al., 1995) through a specially designed field experiment. Comparing measured responses of unfrozen and frozen sand has shown that the latter were “distorted” in a particular way while the former were free from IP effects. The inference that the “distortion” was due to induced polarization was supported by galvanic measurements at early times. Very strong early-time galvanically induced polarization of frozen unconsolidated rocks, both in laboratory and in the field, was reported recently by Ageev (2011).

Although IP-affected transients have been measured in Yakutia since the 1970s, their inversion remained impossible until recently before the appropriate software has appeared. The codes for inversion of the TEM data in terms of frequency dependent conductivity allowed estimating the polarization parameters of rocks in western Yakutia (Kozhevnikov and Antonov, 2006, 2008; Stognii, 2008; Stognii and Korotkov, 2010) where TEM surveys are used for geological mapping and kimberlite exploration.

The next step in studying inductively induced polarization (IIP) in permafrost areas should consist in interpreting the

* Corresponding author.

E-mail address: KozhevnikovNO@ipgg.nsc.ru (N.O. Kozhevnikov)

estimated polarization parameters in terms of rock physics and/or electrodynamics, or, explaining *why* do IP effects show up in TEM data from frozen rocks.

How inductive IP arises

The best way to illustrate how inductive IP arises is by an example of a weakly polarizable conductive ground (Flis et al., 1989; Kozhevnikov and Antonov, 2009a). Figure 1 shows an ungrounded loop (1) with steady current in it. The loop lies on a ground with the dc conductivity σ_0 . As the transmitter current is turned off at the time $t=0$, the primary magnetic field \mathbf{B}_1 instantly goes to zero. This change in \mathbf{B}_1 induces vortex currents to circulate in the ground with their field \mathbf{B}_2 similar to \mathbf{B}_1 at early times. The vortex currents within some rock volume 2 consist of free charges 3 (ions) that move under the action of applied electric field \mathbf{E} . The vortex currents density \mathbf{j}_{cond} is controlled by the conductivity σ_0 .

Assume that a small “inclusion” (4) in the volume 2 contains some bound charges, i.e., is polarizable. If, as it is assumed, the rock chargeability is low, the conduction current distribution and, correspondingly, the field \mathbf{E} remain governed by the conductivity σ_0 . The “inclusion” that bears bound charges polarizes in response to the applied electric field \mathbf{E} . In the case being considered, the effect of \mathbf{E} is to induce the polarization (or *displacement*) currents \mathbf{I}_{pol} in 4, \mathbf{I}_{pol} being proportional to the rate of the \mathbf{E} decay. Like the eddy currents, the polarization currents induce a magnetic field which contributes to the total TEM response.

At early times, the polarization currents have the same direction as the eddy currents (Fig. 1, *b*), but then \mathbf{I}_{pol} come to zero as the polarization process stops at some time when further separation of the bound charges is no longer possible (Fig. 1, *c*).

Once the eddy currents become orders of magnitude lower as a result of heat loss, there is no longer electric field forcing the bound charges to separate (Fig. 1, *d*) and they return to their equilibrium distribution, i.e., there arise polarization currents opposite in direction to the initial one (Fig. 1, *b*). At that stage, the magnetic field of polarization currents has the polarity opposite to that resulting from the “normal” eddy currents.

The ‘inclusions’ with bound charges may represent various objects: electron-conducting mineral grains in ion-conducting rock, or systems of electrolyte-filled pores of different sizes, or an electrical double layers on pore walls and around clay particles, or ice inclusions, etc.

Note that the IP contribution to the TEM response of conductive, polarizable ground or a polarizable object depends on the relative decay rates of the conduction and polarization currents. If the polarization currents decay faster than the conduction ones, the former can show up only as a small perturbation against the latter. Otherwise, the conduction currents decay faster but this short time is *enough* for a system of slowly decaying polarization currents to form under the action of vortex electric field \mathbf{E} . After the eddy currents have

disappeared, the polarization current at any one point of the ground flows in the direction opposite to the direction that eddy current had at the same point. Thus, the polarization currents make a ‘mirror image’ of the early-time conduction currents (Smith et al., 1988).

Phenomenological models of frequency dispersion in rocks

Forward modeling and inversion of TEM responses is most often made first in the frequency domain, and the results are then transformed into the time domain. Fast decaying induced polarization is taken into account via the Cole–Cole complex frequency-dependent conductivity $\sigma^*(\omega)$ (Flis et al., 1989; Lee, 1981; Pelton et al., 1978; Svetov et al., 1996; Wait, 1982):

$$\sigma^*(\omega) = \sigma_0 \frac{1 + (j\omega\tau)^c}{1 + (1-m)(j\omega\tau)^c}, \quad (1)$$

where $j = \sqrt{-1}$; ω is the angular frequency, in $\text{rad} \cdot \text{s}^{-1}$; σ_0 is the dc conductivity, in S/m; m is the chargeability, ($0 \leq m \leq 1$); τ is the IP relaxation time constant, in s; c is the exponent ($0 \leq c \leq 1$, 1 and 0 corresponding, respectively, to a single relaxation time and to an infinitely broad uniform distribution of relaxation times).

The chargeability m is

$$m = \frac{\sigma_\infty - \sigma_0}{\sigma_\infty},$$

where σ_0 is the dc conductivity (commonly measured at frequencies much below the relaxation frequency $\omega_0 = \tau^{-1}$) and σ_∞ is the conductivity at a frequency much higher than ω_0 .

Frequency dispersion is given by (1) assuming that the dielectric permittivity does not depend on frequency and causes no influence on the measured signals. On the other hand, as it was shown earlier (Kozhevnikov and Antonov, 2006; Kozhevnikov and Artemenko, 2004), the use of equation (1) at frequencies corresponding to the spectra of TEM responses is equivalent to an alternative model which combines σ_0 and frequency-dependent dielectric permittivity.

The Cole–Cole complex dielectric permittivity is (Hippel, 1954; Frolov, 1998)

$$\varepsilon^*(\omega) = \varepsilon_0 \left[\varepsilon_\infty + \frac{\varepsilon_s - \varepsilon_\infty}{1 + (j\omega\tau)^c} \right], \quad (2)$$

where ε_0 is the free-space dielectric constant (8.854×10^{-12} F/m); ε_s , ε_∞ are the relative static and dynamic permittivities, respectively; τ is the time constant of dielectric relaxation, in seconds, and c is the exponent. Fast-decaying polarization is described in this way in laboratory dielectric permittivity measurements on frozen ground samples (Bittelli et al., 2004; Frolov, 1998); the case of $c = 1$ corresponds to the Debye relaxation.

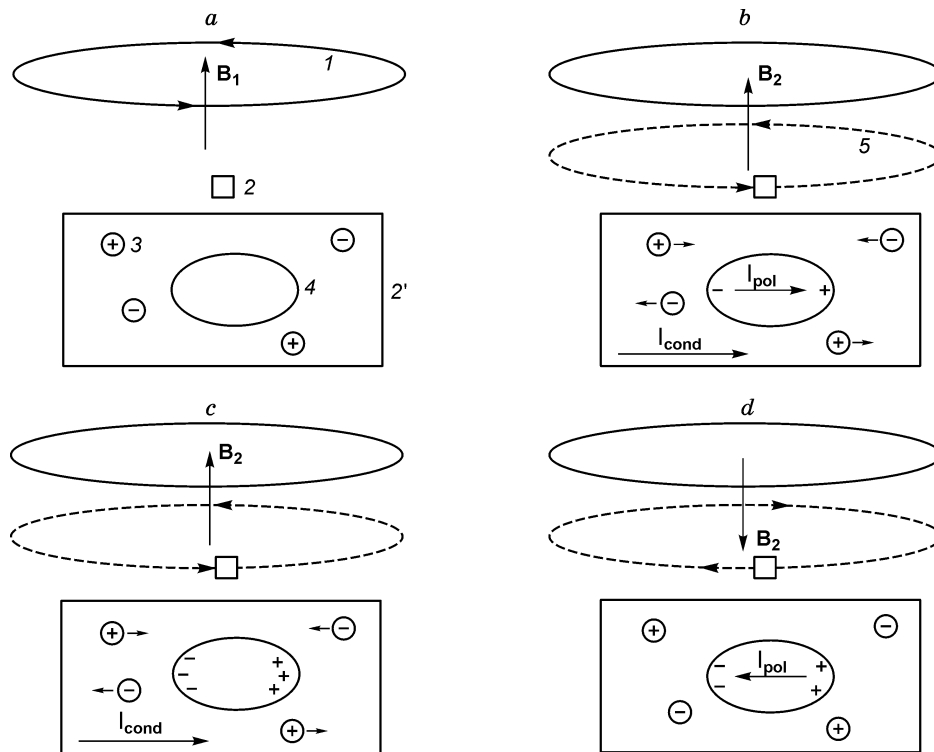


Fig. 1. Inductive IP in rocks. Prior to the turn-off of transmitter current, free and bound charges are distributed evenly and current in the ground is zero (a). As the current in the transmitter loop is turned off, and some time after that, both free and bound charges move making a positively directed current flowing in the ground (b). The bound charges stop splitting at some time, and the polarization current becomes zero (c). At late times, the vortex electric field decreases and becomes unable of maintaining the separating of bound charges which, returning to the equilibrium, produce polarization current flowing in the opposite direction (d). I is the transmitter loop; 2 is a small volume of the medium; 2' is the same volume, enlarged; 3 is a free charge; 4 is a polarizable inclusion; 5 is the current line. B_1 is the primary magnetic field; B_2 is the secondary magnetic field; I_{cond} is the conduction current; I_{pol} is the polarization current.

The conductivity $\sigma^*(\omega)$ of a rock with the dc conductivity σ_0 and the complex permittivity given by (2) is

$$\sigma^*(\omega) = \sigma_0 + j\omega\epsilon_0 \left[\epsilon_\infty + \frac{\epsilon_s - \epsilon_\infty}{1 + (j\omega\tau)^c} \right]. \quad (3)$$

In model (1), it is the chargeability m that measures the capability of a medium to polarize under the applied electric field while in model (2) this is the difference $\Delta\epsilon$ between the relative static and dynamic permittivities ($\Delta\epsilon = \epsilon_s - \epsilon_\infty$) called the dielectric increment (Chelidze et al., 1999). This parameter is free from the effects of the dc conductivity σ_0 , while the chargeability m is subject to both polarization and conductivity controls (Lesmes and Frye, 2001; Lesmes et al., 2005). Normally $\epsilon_\infty \ll \epsilon_s$, $\Delta\epsilon \approx \epsilon_s$, therefore, ϵ_s can be used as a measure of the dielectric response.

In the case of a Debye relaxation ($c = 1$), $\Delta\epsilon$ and m are related as

$$m = \left(1 + \frac{\sigma_0 \tau}{\epsilon_0 \Delta\epsilon} \right)^{-1}, \quad (4)$$

within the frequency range contributing to the spectra of the usual TEM responses (Kozhevnikov and Antonov, 2006; Kozhevnikov and Artemenko, 2004). This means that writing the polarizability via the frequency-independent conductivity

σ_0 and the complex dielectric permittivity $\epsilon^*(\omega)$ following equation (3) at $c = 1$ is equivalent to using the complex frequency-dependent conductivity $\epsilon^*(\omega)$ given by (1) with σ_0 , $c = 1$, and the chargeability m according to (4).

Results: inversion of TEM data from Yakutia

The inversion of transient responses consisted in fitting a 1D layered-earth model to measured data. The IP effects were allowed for by using complex frequency-dependent conductivity of (1). For more details of the procedure and the results see (Kozhevnikov and Antonov, 2006, 2007, 2008, 2009a, 2010; Stognii, 2008; Stognii and Korotkov, 2010).

The inversion of TEM data from Yakutia gave a set of Cole–Cole parameters characteristic of frozen rocks (Table 1): the chargeability m in the range 0.2 to 0.85, most often within 0.2–0.5; the time constant τ from 35 to 250 μs , averaging about 100 μs ; and the exponent c about 0.8 to 1, little variable unlike m and τ .

The fact that in most cases $c \approx 1$ indicates a narrow range of relaxation times and makes the polarization process actually fitting the Debye model. Thus the IP process can be approximated by an exponential decay with a time constant τ , which

Table 1. Parameters of the near-surface polarizable layer found by inversion of TEM responses measured in Western Yakutia (Kozhevnikov and Antonov, 2006, 2008; Stognii, 2008)

Site	ρ , Ohm · m	m	τ , μ s	c	h , m	$\Delta\epsilon$
XXIII CPSU Congress kimberlite pipe	185	0.46	83	0.80	≤ 100	4.3×10^4
Trap quarry, vicinity of Mirnyi	100	0.28	50	0.82	≤ 100	2.2×10^4
Nakyn kimberlite field	20–80	0.20–0.46	35–100	1	10–50	$1.5 \times 10^4 - 2 \times 10^5$
Taezhnaya kimberlite pipe	200	0.55	110	0.85	15	7.6×10^4
Upper Chuonalyr	600	0.70–0.85	170–250	0.80–0.90	≤ 10	$7.5 \times 10^4 - 2.7 \times 10^5$
D'yakhtar	190	0.59	93	0.9	45	8×10^4

allows one to estimate $\Delta\epsilon$ using (4) (see the lower row in Table 1 for the respective values).

Discussion

In this section possible polarization mechanisms are discussed, and the interpretations of the observed IP effects in terms of rock physics are suggested.

As noted above, fast-decaying polarization in frozen ground fits the Debye relaxation with $\tau \approx 100 \mu$ s. According to the published evidence (Frolov, 1998; King and Smith, 1981), this combination of parameters ($c \approx 1$, $\tau \approx 100 \mu$ s) is typical of freshwater polycrystalline ice. Therefore, the fast-decaying IP in permafrost might be associated with dielectric relaxation of ice in the pores.

The relative permittivity of water and ice is (Hippel, 1954; King and Smith, 1981)

$$\epsilon = \epsilon_\infty + \frac{\epsilon_s - \epsilon_\infty}{1 + j\omega\tau} \tag{5}$$

The orientational polarization of water molecules decays fast ($\tau \approx 10^{-11}$ s), but the relaxation time becomes almost six orders of magnitude longer as water freezes to ice (Maeno, 1988; Purcell, 1984). This time (in seconds), for freshwater polycrystalline ice, can be estimated as (King and Smith, 1981)

$$\log \tau = 2900/T - 15.3, \tag{6}$$

where T is the absolute temperature, K. Thus calculated, the relaxation time is $\tau \approx 20 \mu$ s at subzero temperatures and increases to 20 ms when the temperature drops to $-60 \text{ }^\circ\text{C}$. The hypothesis that dielectric relaxation of ice may cause induced polarization of frozen rocks is supported by Stognii (2008) and Stognii and Korotkov (2010). Having compared inverted transient responses with the results of geological and geocryological surveys in Western Yakutia, the cited authors concluded that IP-affected transients occurred over ice-rich shallow sediments.

In order to check the ice dielectric relaxation hypothesis, one has to estimate the magnitude of the effect. It is reasonable to begin with a case when the TEM loop system is laid on massive ice *in situ*, with the ice content 100 vol.% (Fig. 2, a). Inversion of the response measured over an ice massif can be

expected to give values of $\Delta\epsilon = \epsilon_s - \epsilon_\infty \approx \epsilon_s$ common to polycrystalline ice. According to (Frolov, 1998; King and Smith, 1981) for ice $\epsilon_s \approx 100$ which is more than three orders of magnitude lower than the values found from inversion of TEM data (Table 1). Because of this, the IP effects observed in transient responses from Yakutia hardly may result from dielectric relaxation in ice.

Frozen rocks are normally multiphase and heterogeneous, this being their inherent property responsible in many aspects for their formation and changes. Heterogeneous systems, in turn, are remarkable for dielectric dispersion at frequencies different from the respective frequencies of the system's components (Chelidze et al., 1977; Dukhin and Shilov, 1972). One phenomenon contributing to the frequency dependence of dielectric permittivity is the Maxwell–Wagner effect (Hippel, 1954): the electric field charges each interface (even a microscopic one), the charge being proportional to the interface-orthogonal component of the macroscopic electric field and to the difference $(\epsilon_1/\sigma_1) - (\epsilon_2/\sigma_2)$ (Alvarez, 1973; Chelidze et al., 1977). Mathematically, this is an analog of polarization in dielectrics, and that is why the effect is often called “polarization by charge accumulation on the surfaces of inclusions” or *interfacial polarization*.

A large amount of experimental and theoretical work on the Maxwell–Wagner effect has been done for synthetic heterogeneous solids (Chelidze et al., 1977, 1999; Dukhin and Shilov, 1972). The TEM survey people got interested in this effect in search for explanation of the monotony break in TEM responses measured in Yakutia. It was V. Sidorov (Molchanov and Sidorov, 1985; Sidorov, 1985, 1987) who drew attention to the problem and contributed a lot to its formulation. Although remaining within the limits of a flat capacitor model, he was the first to approach the low-frequency permittivity

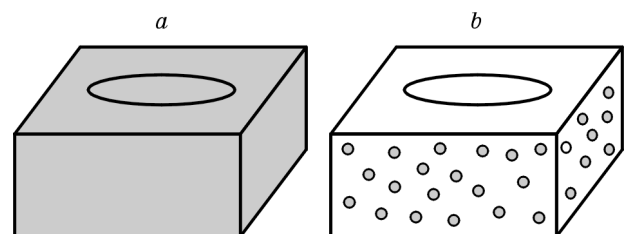


Fig. 2. Ungrounded horizontal loop on the surface of: (a) an ice massif, and (b) a rock with ice inclusions.

dispersion of frozen rocks in terms of interfacial polarization. He, together with his co-authors, undertook a pioneering study of the Maxwell–Wagner effect in borehole and in laboratory (Molchanov and Sidorov, 1985).

One can approximately estimate possible $\Delta\epsilon$ due to the Maxwell–Wagner effect in frozen ground with a model of a porphyric rock (Fig. 2, *b*) which is simple enough not to require too many parameters and yields easily explainable results. Natural frozen rocks that fit this model include those with simple (massive, basal, crust-like, or porphyry-like) cryostructures (Melnikov and Dubikov, 1986).

In permittivity calculations, porphyric heterogeneous solids are considered as two-phase mixtures comprising a continuous matrix of the dielectric permittivity ϵ_1 with embedded spherical inclusions of the permittivity ϵ_2 (Fig. 2, *b*). One of the known formulas for the permittivity of a mixture belongs to Maxwell. It applies to mixtures with spherical inclusions with their volumetric content (P) assumed to be relatively small (Hippel, 1954):

$$\epsilon = \epsilon_1 \left(1 + 3P \frac{\epsilon_2 - \epsilon_1}{\epsilon_2 + 2\epsilon_1} \right). \quad (7)$$

With the potential character of the electric field in mind, equation (7) can be used to estimate the dielectric permittivity of a two-phase medium with regard to the Maxwell–Wagner effect (Chelidze et al., 1977; Dukhin and Shilov, 1972). According to the Maxwell–Wagner theory, the electric field is not vortex. Although being not true in the general case, this may be a convenient approximation for frequencies at which the electromagnetic wavelengths in any phase are much greater than the linear heterogeneity scale (frozen rocks, with heterogeneities existing as inclusions of interstitial ice, mineral grains, etc., certainly satisfy this condition). The advantage of this approximation is reducing the problem (mathematically) to the static case for ideal dielectrics.

Generally, the matrix and the inclusions have their complex permittivities (ϵ_m^* and ϵ_i^*) and conductivities (σ_m^* and σ_i^*).

Then, for a porphyric rock, it is enough that $\epsilon_1^* = \epsilon_m^* - j \frac{\sigma_m^*}{\omega\epsilon_0}$

and $\epsilon_2^* = \epsilon_i^* - j \frac{\sigma_i^*}{\omega\epsilon_0}$ substituted, respectively, for ϵ_1 and ϵ_2 in

(8). Thus one arrives at Wagner's formula (Dukhin and Shilov, 1972):

$$\epsilon^* = \epsilon_1^* \left(1 + 3P \frac{\epsilon_2^* - \epsilon_1^*}{\epsilon_2^* + 2\epsilon_1^*} \right). \quad (8)$$

Thus found permittivity is complex and frequency-dependent even when the permittivity and conductivity of the matrix and the inclusions do not depend on frequency. With the separated real and imaginary parts, respectively, equation (8) becomes $\epsilon^* = \epsilon' - j\epsilon''$.

Obviously, ϵ' presents the effective dielectric permittivity ϵ_{eff} of a mixture while ϵ'' gives its effective conductivity $\sigma_{\text{eff}} = \omega\epsilon_0\epsilon''$:

$$\epsilon^* = \epsilon_{\text{eff}} - j \frac{\sigma_{\text{eff}}}{\omega\epsilon_0}.$$

A frozen rock, in which the mechanisms other than the Maxwell–Wagner effect are minor, is a good model to estimate the order of magnitude of the interfacial polarization. Consider massive frozen sand dielectric relaxation in which was studied intensively in laboratory (Frolov, 1998; Frolov and Fedyukin, 1983) and observed in the field (Kozhevnikov et al., 1995). Almost all interstitial water in sand, as well as in any coarse porous rock, turns into ice already at subzero temperatures. Only its small portion (1–2% or less) remains unfrozen as inclusions and thin films which make up a quasi-continuous matrix with the conductivity σ_1 of the order of 10^{-5} – 10^{-3} S/m (Frolov, 1998; King et al., 1988).

Taking into account that bound water has much less dielectric permittivity than free water (Dukhin and Shilov, 1972) and its volumetric percent is low in coarse frozen rocks, the permeability of the quasi-continuous matrix must be mainly controlled by the permeability of mineral grains. Therefore, one can assume that frozen sand has $\epsilon_1 \approx 5$. As for the inclusions, their dielectric permittivity, ϵ_2^* , was assumed to fit the Debye model (6) and the conductivity, σ_2 , to be in the range 10^{-6} – 10^{-4} S/m.

See the frequency dependence of the effective permittivity in the wet frozen sand model consisting of a continuous matrix with $\epsilon_1 = 5$, $\sigma_1 = 10^{-4}$ S/m and inclusions with $\epsilon_{2s} = 100$, $\epsilon_{2\infty} = 4$, $\sigma_2 = 10^{-5}$ S/m in Fig. 3, *a*. The dependences of ϵ_{eff} on frequency, f , are plotted for the relaxation times τ from zero to 100 μs . According to (6), $\tau_2 = 30 \mu\text{s}$ corresponds to the temperature $-5 \text{ }^\circ\text{C}$ and 100 μs to $-15 \text{ }^\circ\text{C}$. The plots in Fig. 3, *a* show that the effective time of dielectric relaxation of the model increases proportionally to the relaxation time of ice inclusions.

Figure 3, *b* demonstrates how the ice conductivity influences the effective permittivity ϵ_{eff} of the frozen sand model. As σ_2 decreases, the low-frequency values of ϵ_{eff} increase; this increase is first rapid but then, after saturation at $\sigma_2 < 10^{-5}$ S/m, the low-frequency permittivity remains almost invariable. For the $\epsilon_m(f)$ plots of Fig. 3, *b*, the effective relaxation time of the model is 20–34 μs , at a constant relaxation time of the inclusions ($\tau_2 = 30 \mu\text{s}$).

Figure 3 indicates that modeling with regard to the Maxwell–Wagner effect in a porphyric frozen rock predicts frequency dependence of system's permittivity in a frequency range corresponding to the spectra of the TEM responses usually measured in cold regions. However, the dielectric increment $\Delta\epsilon \approx \epsilon_s$, that accounts for the *amplitude* of the frequency dielectric response, is four orders of magnitude lower than that found through inversion of TEM data (Table 1).

Mind that the plots of Fig. 3 were drawn assuming an ice content of $P = 0.1$, though it may reach 50% or more in the upper frozen ground of Western Yakutia (Klimovsky and Gotovtsev, 1994). The use of Maxwell's formula at $P > 0.3$ may lead to large errors, but this does not matter when

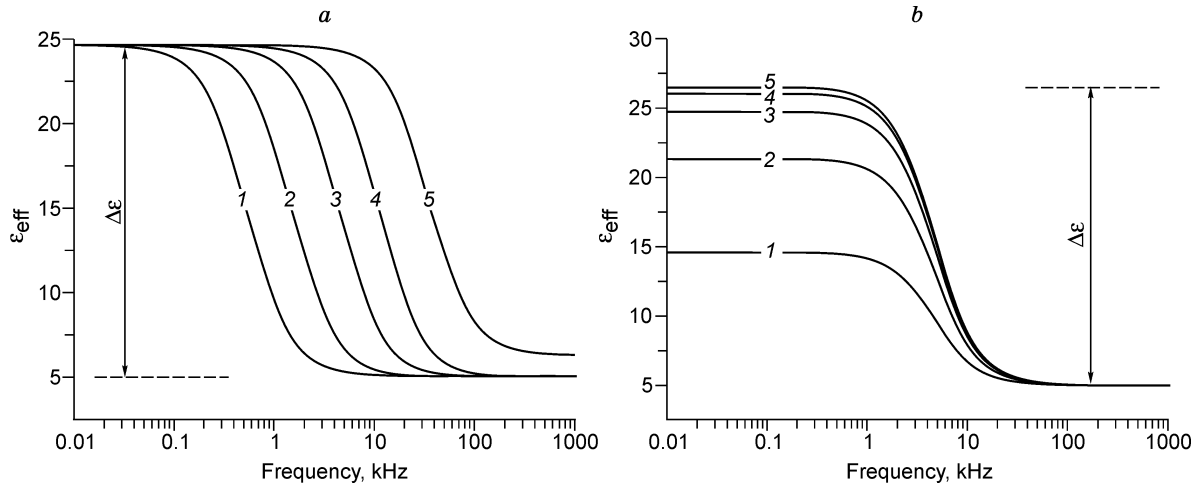


Fig. 3. Frequency dependencies of effective dielectric permittivity of a frozen sand with regard to Maxwell–Wagner effect at different τ_2 (a): 1, 300; 2, 100; 3, 30; 4, 10; 5, 0 μ s; (other parameters: $\sigma_1 = 10^{-4}$ S/m; $\epsilon_1 = 5$; $\sigma_2 = 10^{-5}$ S/m; $\epsilon_{2s} = 100$; $\epsilon_{2\infty} = 4$; $P = 0.1$) and the conductivity of the inclusions σ_2 (b): 1, 10^{-4} ; 2, 3×10^{-5} ; 3, 10^{-5} ; 4, 3×10^{-6} ; 5, 10^{-6} S/m; (other parameters: $\sigma_1 = 10^{-4}$ S/m; $\epsilon_1 = 5$; $\epsilon_{2s} = 100$; $\epsilon_{2\infty} = 4$; $\tau_2 = 30 \mu$ s; $P = 0.1$).

estimating the order of magnitude of the expected effects. One can assume ϵ_s to be approximately proportional to the volumetric content of inclusions. Then, at $P = 50\%$, one may expect $\Delta\epsilon \approx 100$, which is more than thousand times as low as the values given in Table 1.

In (Artemenko and Kozhevnikov, 1999), dielectric permittivities calculated using (8) were compared with laboratory data for frozen rocks (Frolov, 1998). Frozen sand has $\Delta\epsilon$ several times that found with (8) at temperatures below zero but the measured and calculated data agree well at $-15 \text{ }^\circ\text{C}$. Yet, neither the misfit (at about $0 \text{ }^\circ\text{C}$) nor the fit (at $-15 \text{ }^\circ\text{C}$) between the measured and calculated values matter when estimating the order of magnitude of the effects: $\Delta\epsilon$ values measured on frozen sand samples is within a few hundreds (at $\sim 40 \text{ vol.}\%$ water). Therefore, both model and laboratory estimates are at least thousand times different from those found through inversion of TEM data (Table 1).

Thus, dielectric relaxation in ice and/or the Maxwell–Wagner polarization cannot account for the high dielectric increment predicted by the TEM inversion results. That is why electrochemical polarization at the solid (mineral matrix)–liquid (interstitial water) interface is a more likely candidate for the cause of the conductivity and/or permittivity frequency response of frozen ground (Kozhevnikov, 2011).

The surface contribution to processes associated with electrochemical polarization is known to have several controls (Chelidze and Gueguen, 1999): (1) the surface-to-volume ratio (specific surface area) of the components; (2) the surface and volume physical and chemical properties of the components; (3) the mode of coupling between surface and volume processes; (4) the characteristics of the electrical double layer (EDL) at the solid–liquid interface; (5) the geometrical, chemical, or electrical heterogeneity of the interfaces.

Obviously, a water-bearing frozen rock can polarize under a great variety of the above controls. Taking them all into account in a polarization model of frozen ground, with all

their interactions, is obviously a challenge to be met in the future.

In this respect, an alternative model may be of interest in which the complex conductivity of a rock is a sum of bulk and surface conductivities (Lesmes and Friedman, 2005; Lesmes and Frye, 2001; Slater and Lesmes, 2002; Vinegar and Waxman, 1984), which corresponds to the case of parallel conduction paths. The effective conductivity of a small rock volume or sample shown as a parallel equivalent circuit in Fig. 4, a is

$$\sigma^*(\omega) = (\sigma_{\text{bulk}} + j\omega\epsilon_\infty) + (\sigma'_{\text{surf}}(\omega) + j\sigma''_{\text{surf}}(\omega)), \quad (9)$$

where σ_{bulk} and ϵ_∞ are the bulk (low-frequency) conductivity and the high-frequency dielectric permittivity of the bulk rock sample, and $\sigma'_{\text{surf}}(\omega)$ and $\sigma''_{\text{surf}}(\omega)$ are the real and imaginary surface conductivity components. Combining the real and imaginary components in (9) gives

$$\sigma^*(\omega) = [\sigma_{\text{bulk}} + \sigma'_{\text{surf}}(\omega)] + j[\omega\epsilon_\infty + \sigma''_{\text{surf}}(\omega)].$$

Since $\omega\epsilon_\infty \ll \sigma''_{\text{surf}}(\omega)$, at low frequencies where IP processes are commonly measured in the field, the effective conductivity is

$$\sigma^*(\omega) = [\sigma_{\text{bulk}} + \sigma'_{\text{surf}}(\omega)] + j\sigma''_{\text{surf}}(\omega).$$

The imaginary component of conductivity, within the limits of the discussed model and within the frequency range common to the TEM signals spectra, is controlled by the surface conductivity. As for the real conductivity component, it includes the contributions from both bulk and surface conductivities. The vector diagram in Fig. 4, b shows the relationship between the real and imaginary conductivity components and the phase shift (θ).

The bulk rock properties σ_{bulk} and ϵ_∞ are independent of frequency and can be derived from the HB (Hanai–Brugge-

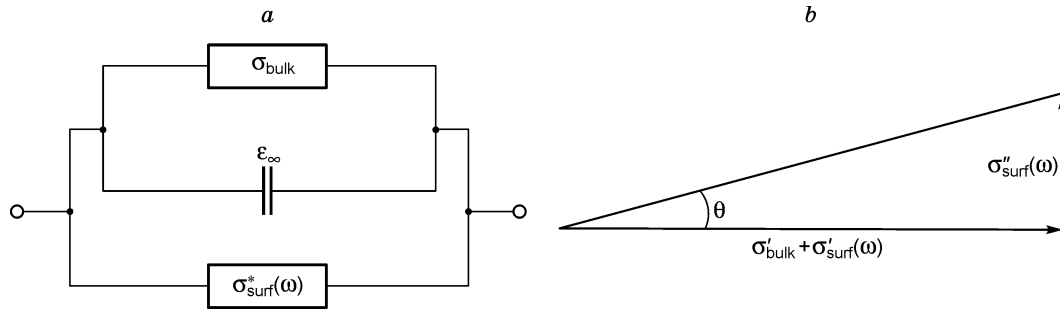


Fig. 4. *a*: Parallel equivalent circuit presentation of rock conductance (Lesmes and Frye, 2001; Vinegar and Waxman, 1984). The bulk conductivity σ_{bulk} of electrolyte in pores does not depend on frequency and causes no capacitance effects. The high-frequency dielectric permittivity defines capacitance of the system at high frequencies. The IP effects are attributed to the imaginary component $\sigma''_{\text{surf}}(\omega)$ of the frequency-dependent complex surface conductivity $\sigma^*_{\text{surf}}(\omega) = \sigma'_{\text{surf}}(\omega) + j\sigma''_{\text{surf}}(\omega)$. *b*: Relationship of the phase angle with the real and imaginary components of the complex conductivity.

man) effective medium theory (Lesmes and Friedman, 2005). The HB low-frequency conductivity is given by

$$\sigma_{\text{bulk}} = \sigma_w \phi^n,$$

where σ_w is the conductivity of the pore solution (interstitial water), ϕ is the porosity, and n is the cementation index which is a function of the effective grain shape. This relationship was first derived empirically by Archie (1942). The high-frequency HB dielectric permittivity is (Lesmes and Friedman, 2005):

$$\epsilon_{\infty} = \epsilon_w \phi^n \left(\frac{1 - \epsilon_{\text{mg}}/\epsilon_w}{1 - \epsilon_{\text{mg}}/\epsilon_{\infty}} \right)^n,$$

where ϵ_w and ϵ_{mg} are the dielectric permittivities of the pore solution and mineral grains, respectively.

Electrochemical polarization at the solid–fluid interface causes the frequency dependence of the complex conductivity $\sigma^*_{\text{surf}}(\omega)$. When $\omega \rightarrow 0$, the permittivity approaches ϵ_s , the imaginary component of the surface conductivity tends to zero while the in-phase conductivity tends to the constant value = $\sigma'_{\text{surf}}(0)$. The dc component of the surface conductivity is given by (Lesmes and Frye, 2001)

$$\sigma'_{\text{surf}}(0) = \lim_{\omega \rightarrow 0} \sigma'_{\text{surf}}(\omega) = \frac{e \mu_s \Sigma_0 S_0}{f_g},$$

where e is the electron charge, μ_s is the effective surface ionic mobility, Σ_0 is the mineral surface charge density, S_0 is the weighted surface-to-volume ratio, f_g is a geometric factor that characterizes the tortuosity of the grain/pore interface.

According to (Lesmes and Frye, 2001), the complex surface conductivity response at an arbitrary frequency can be written as a product of the dc surface conductivity and a spectral response function $J(\omega, g(r), \mu_s)$:

$$\sigma^*_{\text{surf}}(\omega) = \frac{e \mu_s \Sigma_0 S_0}{f_g} J^*(\omega, g(r), \mu_s),$$

where $J^*(\omega, g(r), \mu_s)$ is obtained by convolving the electrochemical polarization response of the fixed and diffuse EDL

parts for a single grain/pore surface with the radius r and the distribution $g(r)$ of the grain/pore sizes. The magnitude of the complex conductivity response is defined primarily by the product of S_0 , Σ_0 , and μ_s , while its frequency dependence is a function of the grain/pore size distribution (Lesmes and Frye, 2001).

Figure 5, which is a schematic version of Fig. 6 from (Lesmes and Frye, 2001), illustrates the frequency dependence observed in laboratory experiments with Berea sandstone saturated with various solutions. These data illustrate the main features of complex conductivity frequency response observed on wet porous rocks. Two upper panels (*a* and *b*) of the figure give, respectively, the plots of $\sigma' = \sigma_{\text{bulk}} + \sigma'_{\text{surf}}$, and $\sigma'' = \sigma''_{\text{surf}}$, and the panel (*c*) shows the behavior of the real permittivity (ϵ') plotted as a function of frequency. The real dielectric permittivity, is related with the imaginary conductivity as

$$\epsilon' = \frac{\sigma''}{\omega \epsilon_0}. \quad (10)$$

At low frequencies (0.01 Hz and less), σ'' tends to zero when $\omega \rightarrow 0$, while ϵ' remains almost invariable approaching asymptotically the low-frequency limit ϵ'_s . Above 0.1 MHz ϵ' tends to the high-frequency limit (ϵ'_{∞}) and σ'' increases proportionally to frequency.

The real permittivity within the frequency range typical of the TEM signals spectra (Fig. 5, *c*) is similar in the order of magnitude to $\Delta\epsilon$ values inferred from the Yakutian TEM data (Table 1). Thus, the surface conductance model may account for the exceptionally high low-frequency dielectric permittivities recovered from the inversion of TEM data.

Inasmuch as porous sedimentary rocks are of broad occurrence everywhere, it is reasonable to question why it is Yakutia where from the IP effects in TEM data are so largely reported? A plausible explanation may be that the contributions of surface and bulk conductivities to a total response are very different depending on whether the same rock is frozen or not.

Figure 6, *a* shows a small rock volume with mineral grains and pore fluid. At positive temperatures, the conductive fluid

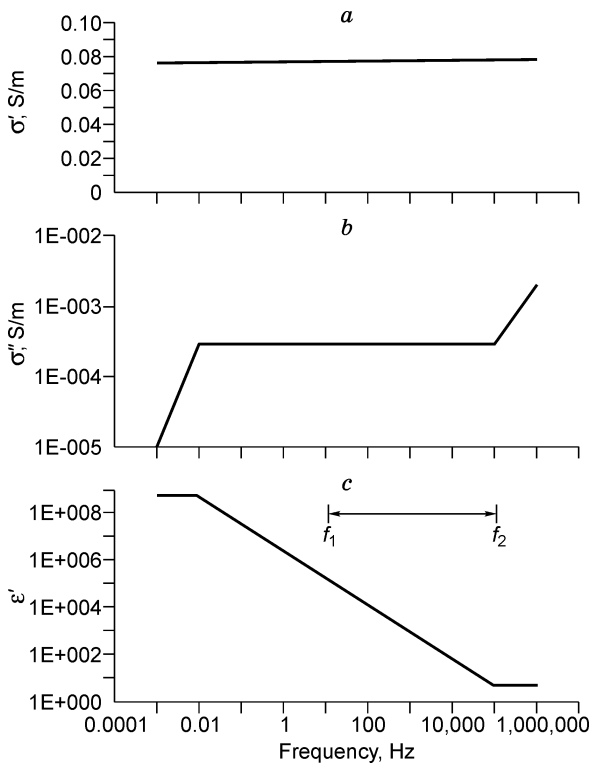


Fig. 5. The real (a) and imaginary (b) components of conductivity, and the real component of dielectric permittivity (c) of water-saturated Berea sandstone as a function of frequency: simplified version of Fig. 6 from (Lesmes and Frye, 2001). Horizontal line with arrows in (c) shows the usual field bandwidth ($f_1 \approx 10$ Hz, $f_2 \approx 10^5$ Hz) typical of the TEM signals spectra.

fills the whole interstitial space, and the bulk conductivity predominates over the surface one ($\sigma'' \ll \sigma'$); the polarizability proportional to $\arctan(\sigma''/\sigma') \approx (\sigma''/\sigma')$ (Slater and Lesmes, 2002) is low, and the IP effects are weak, correspondingly.

At subzero temperatures, the pore water freezes and only its minor portion remains unfrozen in the adsorbed form as thin films on grain/iced pore interfaces (Fig. 6, b). Thereby the bulk conductivity strongly decreases and the rock conductivity becomes tens or hundreds times lower (Frolov, 1998; King et al., 1988). Unlike the bulk conductivity, the surface conductivity depends on the surface-to-volume ratio of the pores which does not change as the rock freezes up. Moreover, inasmuch as the processes at the ice–water interface are the same as at the mineral–water interface (Deryagin et al., 1989; Nechaev and Ivanov, 1974), it is reasonable to expect that interstitial water freezing would increase the surface-to-volume ratio at least twice (Fig. 6, b). Finally, one more cause of a greater surface conductivity contribution to the response might be that pore water freezing increases the salinity of the remaining unfrozen fluid (Frolov, 1998; King et al., 1988).

There is another reason why inductive IP effects may appear mostly in the presence of frozen rocks. Formulated in a simplified way, it is as follows. TEM responses of a polarizing ground result from competition between the IP and “normal” (decaying eddy currents) transient processes (Fig. 1). Other things being equal, the relation of the induction and polarization processes depends on the rocks conductivity: the

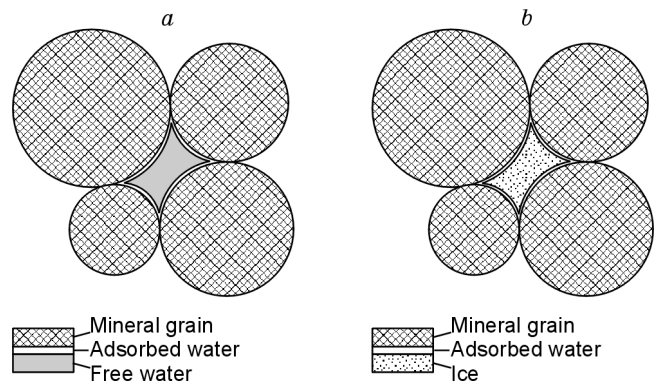


Fig. 6. A small volume of a water-saturated rock at temperatures above (a) and below (b) 0 °C.

lower the conductivity the greater the relative IP contribution to the total response. As a wet rock freezes up, it becomes at least one order of magnitude more resistive, and the IP contribution becomes greater than that of the EM effects. Thus, the IP effects are inconspicuous against the induction ones while the pore water remains unfrozen but as pore water freezes, σ' becomes low, eddy currents decay rapidly, and the total response is due predominantly to the IP effects.

The conclusion that the fast-decaying IP of frozen rocks is electrochemical by its nature follows from necessity to explain very high low-frequency dielectric permittivities obtained through inversion of the TEM data from Yakutia. As things now stand, there are no other feasible causes of anomalously high permittivities except electrochemical polarization of adsorbed water films on grain boundaries.

The above considerations account for the very high low-frequency dielectric response of frozen ground in terms of electrochemical polarization and/or surface conductance. However, one issue remains unexplained. The Cole–Cole exponent $c \approx 1$ indicating the Debye-type relaxation with τ distributed in a narrow range, which follows from inversion of the TEM data, appears to be poorly consistent with the assumed electrochemical nature of polarization and with the fact that near-surface frozen rock in Yakutia may contain a large clay component (Klimovsky and Gotovtsev, 1994). On a laboratory scale, such rocks usually exhibit broad ranges of relaxation times (Bittelli et al., 2004; Frolov, 1998). The problem might lie with poor laboratory and field exploration of the electric properties of permafrost. The first quantitative estimates of the fast-decaying IP in frozen rocks *in situ* obtained through inversion of TEM data may indicate that the available models of dielectric response based uniquely on laboratory measurements are incomplete.

Note that a frozen rock is in some respects similar to a dry rock with air (or any gas) in its pores (Frolov, 1998), which is likewise conducting due to thin films of bound water. Therefore, one may expect IP effects to arise in transient responses of dry porous rocks as well. This hypothesis is supported, specifically, by TEM data from Fogo Volcano (Descloitres et al., 2000).

Conclusions

TEM data from Yakutia and other cold regions of widespread permafrost often bear IP effects. According to the inversion of TEM data in terms of the Cole–Cole model, polarizable are near-surface frozen rocks.

The transient responses of near-surface frozen ground in Yakutia have the chargeability m in the range 0.2 to 0.85, mostly within 0.2–0.5, and the relaxation time constant from 35 to 250 μs (50 to 100 μs on average), but a much less variable exponent c (0.8 to 1). Most often, $c \approx 1$, which is evidence of a Debye-type relaxation process with a narrow range of relaxation times. Therefore, one can, using (3), convert chargeability into low-frequency relative dielectric permittivity found to be tens or a few hundreds of thousands.

The fact of the exponent being $c \approx 1$ suggests that the fast-decaying polarization in permafrost might be due to dielectric relaxation of pore ice and/or to the interfacial polarization. Both models predict a Debye relaxation of frozen rocks within the frequency range characteristic of the TEM signals spectra, but the dielectric increment implied by those models is three or four orders of magnitude lower than the values recovered through inversion of the Yakutian TEM data.

A most likely reason of very high $\Delta\epsilon$ values is electrochemical polarization of the films of unfrozen water that stays adsorbed on the surfaces of mineral grains and inclusions as the rock freezes.

It is convenient to represent the electrochemical polarization effects in terms of frequency-dependent surface conductivity related with the surface-to-volume ratio.

There are two reasons why inductive IP effects may appear over permafrost so often. One explanation, in terms of rock physics, is that the surface conductance remains inconspicuous against the bulk one while pore fluid is unfrozen in the rock and the latter is low polarizable. However, upon transforming the interstitial water into ice, the bulk conductance tends to zero while the surface one remains invariable or increases thus increasing the chargeability. The other cause is in the EM nature: the relative contribution of the eddy currents becomes less than that of IP currents as a result of the abrupt drop in the bulk conductivity upon freezing.

The fact that, according to the inversion of the TEM data, fast-decaying IP in frozen ground is described by the Cole–Cole model with $c \approx 1$ is in rather poor agreement with the assumed electrochemical nature of IP effects. It may indicate the imperfectness of the available theoretical and experimental models and the necessity for further laboratory and field investigation into the nature of induced polarization in frozen rocks.

References

Ageev, V.V., 2011. Laboratory-scale induced polarization measurements on frozen rock samples, in: Proc. V All-Russian M.N. Berdichevsky and L.L. Vanyan Workshop on Electromagnetic Sounding of the Earth: EMS-2011, St. Petersburg, 16–21 May 2011 (in 2 Volumes). St. Petersburg University, Vol. 2, pp. 11–14.

Alvarez, R., 1973. Complex dielectric permittivity in rocks: a method for its measurement and analysis. *Geophysics* 38 (5), 920–940.

Archie, G.E., 1942. The electrical resistivity log as an aid in determining some reservoir characteristics. *Trans. Am. Inst. Mining Metallurgical and Petroleum Engineers* 146, 54–62.

Artemenko, I.V., Kozhevnikov, N.O., 1999. Modeling the Maxwell–Wagner effect in porphyric frozen ground. *Kriosfera Zemli* III (1), 60–68.

Bittelli, M., Flury, M., Roth, K., 2004. Use of dielectric spectroscopy to estimate ice content in frozen porous media. *Water Resour. Res.* 40, W04212 (1–11), doi:10.1029/2003WR002343.

Chelidze, T.L., Gueguen, Y., 1999. Electrical spectroscopy of porous rocks: a review-1. Theoretical models. *Geophys. J. Int.* 137, 1–15.

Chelidze, T.L., Derevyanko, A.I., Kurilenko, O.D., 1977. Electric Spectroscopy of Heterogeneous Systems [in Russian]. Naukova Dumka, Kiev.

Chelidze, T.L., Gueguen, Y., Ruffet, R., 1999. Electrical spectroscopy of porous rocks: a review-2. Experimental results and interpretation. *Geophys. J. Int.* 137, 16–34.

Deryagin, B.V., Kiseleva, O.A., Sobolev, V.D., 1989. Flow of unfrozen water in porous solids, in: Deryagin, B.V., Churaev, N.V., Ovcharenko, F.D. (Eds.), *Water in Disperse Systems* [in Russian]. Khimiya, Moscow, pp. 101–115.

Descloitres, M., Guerin, R., Albouy, Y., Tabbagh, A., Ritz, M., 2000. Improvement in TDEM sounding interpretation in presence of induced polarization. A case study in resistive rocks of the Fogo volcano, Cape Verde Islands. *J. Appl. Geoph.* 45, 1–18.

Dukhin, S.S., Shilov, V.N., 1972. Dielectric Effects and Electric Double Layer in Disperse Systems and Poly-Electrolytes [in Russian]. Naukova Dumka, Kiev.

Flis, F.M., Newman, G.A., Hohman, G.W., 1989. Induced-polarization effects in time-domain electromagnetic measurements. *Geophysics* 54, 514–523.

Frolov, A.D., 1998. Electric and Elastic Properties of Permafrost and Ice [in Russian]. ONTI PNTs RAN, Puschino.

Frolov, A.D., Fedyukin, I.V., 1983. Polarization of frozen disperse rocks in transient electric fields. *Izv. Vuzov. Geologiya i Razvedka*, No. 6, 90–96.

Hippel, A.R., 1954. *Dielectrics and Waves*. John Wiley & Sons, New York.

King, R., Smith, G., 1981. *Antennas in Matter: Fundamentals, Theory and Applications*. MIT Press, Cambridge, MA.

King, M.S., Zimmerman, R.W., Corwin, R.F., 1988. Seismic and electrical properties of unconsolidated permafrost. *Geoph. Prosp.* 36, 349–364.

Klimovsky, I.V., Gotovtsev, S.P., 1994. The Permafrost Zone of the Yakutian Diamond Province [in Russian]. Nauka, Novosibirsk.

Kozhevnikov, N.O., 2011. Surface conductivity in sediments and its relation with induced polarization, in: Erofeev, L.Ya., Isaev, V.I. (Eds.), *Geophysical Methods in Exploration* [in Russian]. Tomsk Technological University, Tomsk, pp. 49–52.

Kozhevnikov, N.O., Antonov, E.Y., 2006. Fast-decaying IP in frozen unconsolidated rocks and potentialities for its use in permafrost-related TEM studies. *Geophysical Prospecting* 54, 383–397.

Kozhevnikov, N.O., Antonov, E.Y., 2007. Fast-decaying IP in unconsolidated frozen ground: An inversion numerical experiment for a uniform polarizable earth. *Geofizika*, No. 1, 42–50.

Kozhevnikov, N.O., Antonov, E.Yu., 2008. Inversion of TEM data affected by fast-decaying induced polarization: Numerical simulation experiment with homogeneous half-space. *J. Applied Geophysics* 66, 31–43.

Kozhevnikov, N.O., Antonov, E.Yu., 2009a. Frequency induction soundings of polarizable earth. *Geofizicheskii Zhurnal* 31 (4), 104–118.

Kozhevnikov, N.O., Antonov, E.Yu., 2009b. Joint inversion of IP-affected TEM data. *Russian Geology and Geophysics (Geologiya i Geofizika)* 50 (2), 136–142 (181–190).

Kozhevnikov, N.O., Antonov, E.Yu., 2010. Inversion of IP-affected transient responses of a two-layer earth. *Russian Geology and Geophysics (Geologiya i Geofizika)* 51 (6), 708–718 (905–918).

Kozhevnikov, N.O., Artemenko, I.V., 2004. Modeling the effect of dielectric relaxation in frozen ground on ungrounded-loop transient responses. *Kriosfera Zemli* VIII (2), 30–39.

Kozhevnikov, N.O., Nikiforov, S.P., Snopkov, S.V., 1995. Fast-decaying IP polarization in frozen ground. *Geoekologiya*, No. 2, 118–126.

- Krylov, S.S., Bobrov, N.Yu., 2002. Frequency dispersion of electrical properties of frozen ground: TEM sounding application. *Kriosfera Zemli* VI (3), 59–68.
- Lee, T., 1981. Transient response of a polarizable ground. *Geophysics* 46, 1037–1041.
- Lesmes, D.P., 2001. Dielectric spectroscopy of sedimentary rocks. *J. Geophys. Res.* 106 (B7), 13,329–13,346.
- Lesmes, D.P., Friedman, Sh.P., 2005. Relationships between the electrical and hydrogeological properties of rocks and soils, in: Rubin, Y., Hubbart, S.S. (Eds.), *Hydrogeophysics*. Springer, Dordrecht, pp. 87–128.
- Lesmes, D.P., Frye, K.M., 2001. Influence of pore fluid chemistry on the complex conductivity and induced polarization response of Berea sandstone. *J. Geophys. Res.* 106 (B3), 4079–4090.
- Maeno, N., 1988. *The Ice Science* [Russian Translation from Japanese]. Mir, Moscow.
- Molchanov, A.A., Sidorov, V.A. (Eds.), 1985. *Polarization of Rocks* [in Russian]. VINITI Reports, No. 5847–85.
- Melnikov, E.S., Dubikov G.I. (Eds.), 1986. *Methods of Regional Engineering-Permafrost Studies for Plainland Terrains* [in Russian]. Nedra, Moscow.
- Nechaev, E.A., Ivanov, I.A., 1974. The electric double layer at the ice-electrolyte interface. *Kolloidnyi Zhurnal* XXXVI, Issue 3 (May–June), 583–584.
- Olenchenko, V.V., Kozhevnikov, N.O., Matrosov, V.A., 2008. Fast-decaying induced polarization of the near-surface frozen rocks of the Mirny kimberlite field: 3rd Saint Petersburg International Conference & Exhibition, 7–10 April 2008. Lenexpo, St. Petersburg, Russia. C010.
- Pelton, W.H., Ward, S.H., Hallof, P.G., Sill, W.R., Nelson, P.H., 1978. Mineral discrimination and removal of inductive coupling with multifrequency IP. *Geophysics* 43, 588–609.
- Purcell, E.M., 1984. *Electricity and Magnetism* (Berkeley Physics Course, Vol. II), second ed. McGraw-Hill.
- Sidorov, V.A., 1985. *TEM Surveys* [in Russian]. Nedra, Moscow.
- Sidorov, V.A., 1987. On electrical chargeability of nonuniform rocks. *Izv. AN SSSR, Fizika Zemli*, No. 10, 58–64.
- Slater, L., Lesmes, D., 2002. IP interpretation in environmental investigations. *Geophysics* 67 (1), 77–88.
- Smith, R.S., Klein, J., 1996. A special circumstance of airborne induced-polarization measurements. *Geophysics* 61, 66–73.
- Smith, R.S., Walker, P.W., Polzer, B.D., West, G.F., 1988. The time-domain electromagnetic response of polarizable bodies: an approximate convolution algorithm. *Geoph. Prosp.* 36, 772–785.
- Stognii, V.V., 2008. Transient electromagnetic prospecting on investigations of induced polarization effects in frozen ground of Yakutian kimberlite province. *Kriosfera Zemli* XII (4), 46–56.
- Stognii, V.V., Korotkov, Yu.V., 2010. *TEM Surveys for Kimberlite Exploration* [in Russian]. Malotirazhnaya Tipografiya 2D, Novosibirsk.
- Svetov, B.S., Ageev, V.V., Lebedeva, N.A., 1996. Polarizability of rocks and high-resolution resistivity surveys. *Geofizika*, No 4, 42–52.
- Vanchugov, V.A., Kozhevnikov, N.O., 1998. Methods and results of TEM soundings for the resistivity structure of the Nakyn kimberlite field (Western Yakutiya), in: Uchitel, M.S. (Ed.), *Geology, Prospecting and Exploration of Mineral Deposits. Collection of Papers* [in Russian]. Irkutsk Technological University, Irkutsk, pp. 164–176 (Transactions of Irkutsk Technological University, Issue 22).
- Vinegar, H.J., Waxman, M.H., 1984. Induced polarization of shaly sands. *Geophysics* 49 (8), 1267–1287.
- Wait, J.R., 1982. *Geo-Electromagnetism*. Academic Press, New York.
- Walker, G.G., Kawasaki, K.K., 1988. Observation of double sign reversals in transient electromagnetic central induction soundings. *Geoexploration* 25, 245–254.

Editorial responsibility: M.I. Epov